Supporting information for the article:

Mechanistic Pathways for Methylcyclohexane Hydrogenolysis over Supported Ir Catalysts

Hui Shi, [1,†] *Oliver Y. Gutiérrez,* [1,*] *Anmin Zheng,* [2] *Gary L. Haller,* [1] *Johannes A. Lercher* [1,*]

[1] *Department of Chemistry and Catalysis Research Center, Technische Universität München, Lichtenbergstraße 4, D-85747 Garching, Germany*

[2] *State Key Laboratory of Magnetic Resonance and Atomic and Molecular Physics, Wuhan Institute of Physics and Mathematics, Chinese Academy of Sciences, Wuhan 430071, China*

[†]*Present address: Pacific Northwest National Laboratory, 902 Battelle Boulevard, P.O. Box 999, MSIN K2-57, Richland, WA 99352, USA*

* Corresponding authors: oliver.gutierrez@mytum.de (O.Y. Gutiérrez); johannes.lercher@ch.tum.de (J.A. Lercher)

Fax: +49 89 28913544; Tel: +49 89 28913540.

S1. Isotope effect: a brief introduction to the theoretical background

For multistep reactions, the kinetic isotope effect (KIE in a general sense) is a composite of the isotope effects for all forward and reverse steps up to and including the rate-determining step (RDS). Quasi-equilibrated steps preceding the RDS manifest equilibrium (or thermodynamic) isotope effects (EIEs). Primary H/D isotope effects, observed when the isotopic substitution is in a chemical bond that is broken or formed in the rate limiting step, are often interpreted by using the two simple guidelines illustrated in Schemes S1 and S2: (i) KIEs for an elementary step are 'normal' ($k_H/k_D > 1$, following the convention of having the light isotope in the numerator) and (ii) EIEs are dictated by deuterium preferring to be located in the site corresponding to the highest frequency oscillator (for ground states, transition states or products) and, as such, may be either 'normal' ($K_H/K_D > 1$) or 'inverse' ($K_H/K_D < 1$). Note that in both cases, the Gibbs free energy (or, potential energy) profiles are presented.

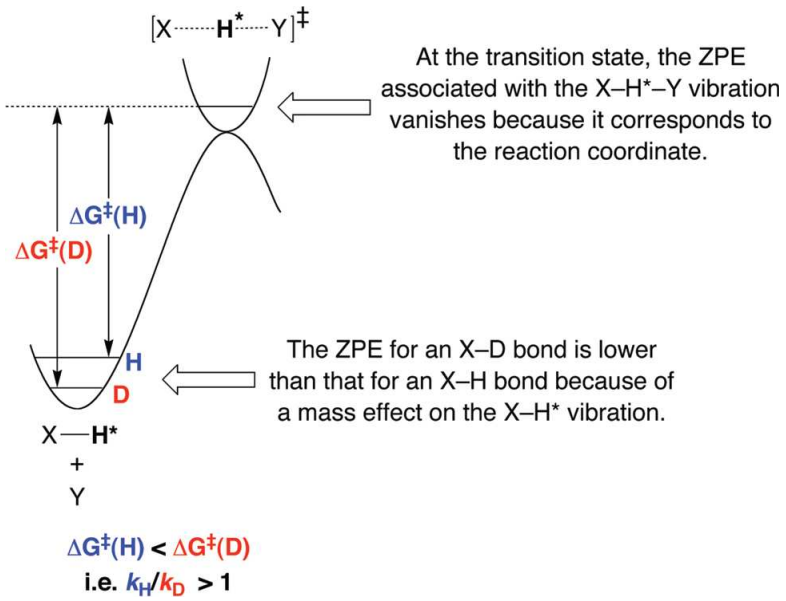

Scheme S1. Simple rationalization of a normal primary KIE (i.e. $k_H/k_D > 1$) for cleaving X−H and X−D bonds [S1]. ZPE is short for zero point energy.

The KIE reflects the zero-point energy (ZPE) difference (or more precisely, free energy difference in Scheme S1) between reactants and transition states when they contain H or D. In a specific elementary step, since D sits at a lower position of the energy well than H,

the activation barrier is higher if the bond containing H or D dissociates in the transition state, resulting in a larger-than-unity ('normal') ratio of rate constants for H- and D-containing species. On the other hand, the EIE reflects the ZPE difference between reactants and products in an elementary step. An important rule is− the higher frequency of the vibrational oscillator is, the larger the ZPE difference will be between H- and D-containing species. Therefore, as is shown in Scheme S2, the change of vibrational frequency from low to high is accompanied with an inverse equilibrium isotope effect. Whether the value is normal or inverse does not depend on the overall energetics (i.e., endothermic or exothermic) of this equilibrated step. It only depends on the relative magnitude of the vibrational frequencies in the H-containing oscillators with reactant (X−H) and with product (Y−H).

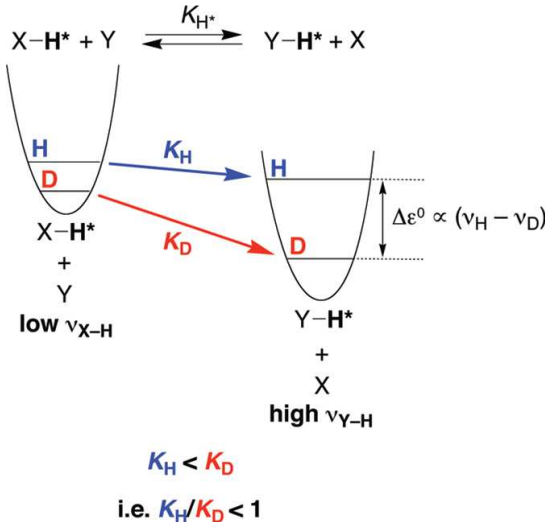

Scheme S2. A simple illustration showing that deuterium prefers to reside in the site that corresponds to the highest stretching frequency (i.e., Y−H* versus X−H*; H* = H, D) [S1].

However, keep in mind that we are here only talking about activation barriers and heat of adsorption, but so far not concerned with the entropy factors from translational, rotational and vibrational movements of the species. In a more rigorous treatment, these entropic factors must be taken into account as they have a good chance of overweighing the enthalpic factors at increasing temperatures. Moreover, unlike homogeneous reactions

where surface coverage effects are not present, the isotope effects from the heterogeneous catalysis is more intricate, because not only kinetic and thermodynamic constants of the elementary steps but also coverages of reactive species might be influenced by isotopic substitution. Therefore, for reactions showing fractional orders in the reactants the evaluation of isotope effects typically becomes very difficult as there is not a single species dominating the site coverage that would simplify the rate equation.

Even in the absence of coverage effects, it represents a grand challenge to predict the isotope effect within a high precision due to the non-availability of thermodynamic data for the surface species, for most of which the structures are unknown. Furthermore, data (such as vibrational frequencies and bond strengths) for gas-phase molecules are often lacking.

Despite all the difficulties, successful examples exist to show that predicting the isotope effect is feasible for simple reactions and specific conditions. Au-Yeung et al. applied a statistical thermodynamics approach to theoretically assessing the kinetic isotope effect (in a general context, KIE refers to the ratio of rate constants, or even more arbitrarily, rates for H- and D-containing species) for the overall reaction, methane (CH_4 or CD_4) oxidation on PdO clusters [S2]. This literature example illustrates how excellent the measured H/D isotope effect and the one predicted from a certain mechanistic sequence could be in agreement with each other. In this light, statistical thermodynamics could be very helpful to the theoretical evaluation of isotope effects, and thus to the elucidation of the elementary steps. The core concepts of statistical mechanics for analyzing isotope effects are described next.

S2. Description of the statistical thermodynamic approach in this study

The evaluation of four types of partition functions (PF) is the core of this approach [S2]. They are translational, rotational, vibrational and electronic PFs. The first three are typically lumped as entropic factors and the last one reflects the zero point energy (ZPE)-corrected activation barrier which in most cases is the dominant influence on isotope effects. Configurational and nuclear PFs do not pertain to the analysis done here of isotope effects.

Rate constant for the reaction between M reactants leading to the transition state (TS):

$$k = \frac{k_B T}{h} \frac{(Q/V)_{TS}'}{\prod_{i=1}^{M} (Q/V)_i} \exp\left(\frac{-E_a}{RT}\right)$$

Equilibrium constant for the reaction between M reactants to form N products:

$$K_{eq} = \frac{\prod_{j=1}^{N} (Q/V)_j}{\prod_{i=1}^{M} (Q/V)_i} \exp\left(\frac{-\Delta E_{rxn}}{RT}\right)$$

where Q/V is the total partition function per unit volume, ΔE_{rxn} is the change in energy of the reaction, E_a is the activation barrier, k_B is the Boltzmann constant, h is the Planck constant, R is the universal gas constant.

Translational partition function: (*per unit volume*)

$$\frac{Q_{trans}}{V} = \frac{(2\pi m k_B T)^{3/2}}{h^3}$$

Rotational partition function: (*for one degree of freedom*)

$$Q_{rot,i} = \frac{k_B T}{hcB_i}$$

(*for three degrees of freedom*)

$$Q_{rot} = \frac{8\pi}{\sigma h^3} (2\pi k_B T)^{3/2} (I_x I_y I_z)^{1/2}$$

Vibrational partition function: *(for one degree of freedom)*

$$Q_{vib,i} = \frac{1}{1 - \exp\left(\frac{-h\nu_i}{k_B T}\right)}$$

Electronic partition function: *(for one degree of freedom)*

$$Q_{elec,i} = \exp\left(\frac{-\varepsilon_0}{k_B T}\right)$$

where m is the mass or reduced mass of the species, B_i is the rotational constant, c is the speed of light, σ is the symmetric number of the molecule or species, $I_{x,y,z}$ is the moment of inertia about the x,y,z axis, ν_i is the vibrational frequency and ε_0 is the zero point energy (ZPE).

Scheme S3. The statistical thermodynamic representations of rate and equilibrium constants and the four categories of partition functions [S3].

According to the representations in Scheme S3, upon replacing a H-atom with a D-atom, the mass difference causes the translational PF to increase. Since the moment of

inertia increases, while the vibrational frequency decreases, with increasing mass/reduced mass, rotational and vibrational PFs also grow with displacement of H with D. Moreover, the vibrational PF is close to unity (1.00−1.01) for wavenumbers larger than 1600 cm^{-1} (e.g., both gaseous H_2, D_2) at T < 1000 K. For molecules that contain isotopically sensitive low-frequency vibrational modes, however, the vibrational PF still plays a role in determining the H/D isotope effects. To evaluate the isotope effects encountered in heterogeneous reactions by a statistical mechanics means, one has to invoke the equations in Scheme S3. Several assumptions have to be made for predicting the isotope effect on the basis of a proposed mechanism (e.g., unperturbed vibrations from a free hydrocarbon to an adsorbed intermediate), due to the insufficient available data regarding some parameters. In this respect, theoretical calculations would be particularly useful for improving the accuracy of predicted isotope effects [S4].

S3. Sequences of steps, rate expressions and theoretical isotope effects for three different mechanisms with different rate-determining steps

Otherwise specified, the site balance equation for derivation of rate expressions is written as: $n\theta_c + m\theta_H + \theta_v = 1$, where θ_c is the coverage of the C-containing intermediates, θ_H is the coverage of hydrogen adatoms (*n* and *m* are the required number of the active site for activation of the two reactants; depending on the identity of the active site, *n* and *m* may vary) and θ_v is the coverage of uncovered active sites. We assume that the adsorption of both dihydrogen and MCH-derived species takes up two contiguous surface atoms.

In the following derivations of rate equations (Section S3.1 to S3.4), we do not propose an exclusive most abundant surface intermediate that dominates over the others in terms of surface coverage and we do not propose that it is also the most reactive among all the intermediates. This makes the mechanisms more general and more powerful in correlating with the experimental data.

S3.1. Group I mechanisms: C–H(D) bond dissociation as the RDS

S3.1.1. Derivation of rate equation for Group I mechanisms

A generalized kinetic sequence is presented in Scheme S4 without showing kinetically

insignificant steps following the RDS. Note that the analysis for a case where the first C–H bond cleavage is rate-determining is presented in Section S3.2.

The vacant site pair (*–*) can be considered as the active ensemble (#) in the kinetic treatment. Note that, although the rate values are reported typically on the basis of exposed surface atoms (*) not site pairs, this treatment does not influence the analyses done for the isotope effects that compare the rate ratios and therefore do not depend on the way of normalizing rates. Moreover, this treatment simplifies the mathematical derivation, which otherwise requires solutions to quadratic equations as reported previously [S5,S6].

(i) H_2 chemisorption:

$$H_2\,(g) + *–* \overset{K_H}{\rightleftharpoons} H{**}H \qquad K_H = \frac{\theta_{H**H}}{P_H \theta_{**}}$$

(where *–* and H**H represent a pair of adjacent free and H*-covered sites; θ_{**}, θ_{H**H} are the corresponding coverages, respectively)

(ii) Hydrocarbon activation (fast steps of C–H bond breaking, lumped with recombination of H^* into gas phase H_2):

$$c\text{-}C_7H_{14}\,(g) + *–* \overset{K_{cyc}}{\rightleftharpoons} (c\text{-}C_7H_{14-2x})** + xH_2\,(g) \qquad K_{cyc} = \frac{\theta_{cyc} P_H^{\,x}}{P_{cyc} \theta_{**}}$$

(where θ_{cyc} and x are the coverage by $(c\text{-}C_7H_{14-2x})**$ and the corresponding depth of dehydrogenation, respectively)

(iii) C–H bond dissociation (rate-determining):

$$(c\text{-}C_7H_{14-2x})** + * \xrightarrow{k_{rds}} (c\text{-}C_7H_{13-2x})** + H* \qquad R_{rds} = k_{rds}\,\theta_{cyc}\,\theta_*$$

(where all the symbols bear the same meanings as mentioned above)

Scheme S4. A generalized kinetic sequence for Group I Mechanisms which assume quasi-equilibrated nature of H_2 dissociation and the C–H bond breaking steps preceding the rate determining C–H bond dissociation. Kinetically irrelevant steps are not shown.

In perpendicular adsorption, a pair of empty sites can only enable at most four hydrogen atoms from the two attaching endocyclic carbons to be removed; the other hydrogen atoms cannot be removed due to the lack of contacts between the surface and other carbon atoms. Flat adsorption can, however, overcome this problem and enable further dehydrogenation, but is most favored on flat surfaces with large ensembles of metal atoms. As a kinetic simplification, we can still treat the flat-lying deeply dehydrogenated species as equivalent to one that requires a pair of sites (e.g., Scheme S5).

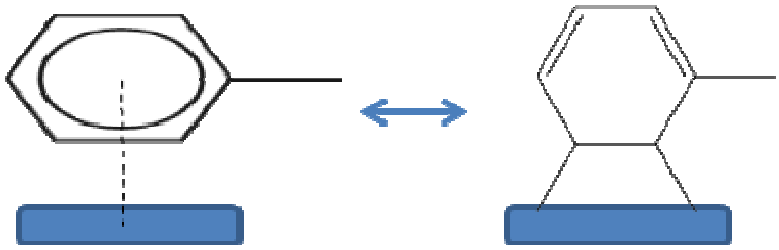

Scheme S5. Proposed kinetic equivalence between a flat-lying species (e.g., adsorbed toluene) and a doubly bound species requiring a pair of unoccupied surface atoms.

A site balance equation applied to the concentrations of all the surface species (the ones that appear after the RDS are negligible in coverage) would give rise to the following:

$$\theta_{cyc,i} = \frac{[C]_i}{[\#]} = \frac{\frac{K_{c,i}P_{cyc}}{P_H^{x_i}}}{1 + K_H P_H + \sum_i \frac{K_{c,i}P_{cyc}}{P_H^{x_i}}} \quad \text{(S1)}$$

where $\theta_{cyc,i}$ is the coverage by the MCH-derived surface intermediate i, [#] is the concentration of the vacant site-pair, $[C]_i$ is the concentration of the MCH-derived intermediate i, and x_i is the dehydrogenation depth of this intermediate, respectively.

$$\theta_{cyc,i} = \frac{[C]_i}{[\#]} = \frac{\frac{K_{c,i}P_{cyc}}{P_H^{x_i}}}{1 + K_H P_H + (K_H' P_H)^{0.5} + \sum_i \frac{K_{c,i}P_{cyc}}{P_H^{x_i}}} \quad \text{(S1')}$$

There would be some changes in the denominator term on the right side of Eq. (S1), leading to Eq. (S1') (see above and Appendix S1), if hydrogen dissociation does not require vacant site pairs or if half H(D)* half vacant site pairs (H*/D*−*) also exist on the surface (due to the mobile nature of and relatively low surface diffusion barriers for surface hydrogen species; the relative abundance of H/D*−* and H**H (D**D) is a statistical function which varies with the number of empty sites and gas phase dihydrogen pressure). But these would not influence the analyses done below in Section S3.1.2. They would, however, affect the kinetic modeling results, which rely on the detailed forms of the coverage term. For the sake of argument, we retain Eq. (S1) for the subsequent analyses, while bearing in mind that both H/D*−* and H**H (D**D) may be present, i.e., $K_H''P_H^m$ ($0.5<m<1$) instead of K_HP_H, under conditions explored in this study where a saturation coverage of hydrogen was not reached.

We do not make *a priori* assumptions that the MCH-derived species other than the one involved in the RDS are much lower in coverages and that there is a unique RDS (even if there are several other irreversible steps that follow the quasi-equilibrated steps, only the rate constant of the first irreversible step appears in the rate expression). To facilitate the discussion, however, the RDS is proposed to be a specific C−H(D) bond dissociation step which has the smallest rate constant of all elementary steps. Therefore, the rate of this reaction, which is governed by the rate of the RDS (step (iii), Scheme S4), can be expressed as:

General rate expression for Group I mechanisms:

$$r_{*-*} = k_{rds,I}\theta_{cyc,rds}\theta_{\#}^{\frac{1}{2}} = \frac{k_{rds,I}\dfrac{K_{c,rds}P_{cyc}}{P_H^{\,x_{rds}}}}{(1+K_HP_H+\sum_i \dfrac{K_{c,i}P_{cyc}}{P_H^{\,x_i}})^{\frac{3}{2}}} \quad \text{(S2)}$$

where $k_{rds,I}$ is the rate constant for the RDS; $\theta_{c,rds}$, $K_{c,rds}$ and x_{rds} are the coverage of the specific intermediate *involved in the RDS*, the dehydrogenation equilibrium constant, and half the number of detached hydrogen atoms (from MCH) to form this intermediate, respectively; the other symbols bear the same meanings as defined in Scheme S4 and Eq.

(S1). The probability factor, not explicitly shown and independent of isotope identity, for finding vacant site pairs or single unoccupied atom is incorporated into either the rate constant or equilibrium constant.

S3.1.2. Derivation of a simple relation between the coverage of hydrocarbon and the measured reaction order

In the following, we derive a straightforward relation between the measured reaction order in MCH, $\frac{\partial \ln(r)}{\partial \ln(P_{MCH})}$, and the coverage by MCH-derived species, based on simple numerical treatment. From Eq. (S2), the reaction order in MCH can be expressed as:

$$\frac{\partial \ln(r)}{\partial \ln(P_{cyc})} = \frac{\partial \ln(\frac{k_{rds}\frac{K_{c,rds}P_{cyc}}{P_H^{x_{rds}}}}{(1+K_HP_H+\sum_i \frac{K_{c,i}P_{cyc}}{P_H^{x_i}})^{\frac{3}{2}}})}{\partial \ln(P_{cyc})} = \frac{\partial \ln(\frac{k_{rds}K_{c,rds}}{P_H^{x_{rds}}}) + \partial \ln(\frac{P_{cyc}}{(1+K_HP_H+\sum_i \frac{K_{c,i}P_{cyc}}{P_H^{x_i}})^{\frac{3}{2}}})}{\partial \ln(P_{cyc})}$$

The first term in the numerator on the right side is independent of P_{cyc}, and therefore will disappear in the derivatives.

Replacing '$1+K_HP_H$' with 'a', and replacing $\sum_i \frac{K_{c,i}}{P_H^{x_i}}$ with 'b', we have:

$$\frac{\partial \ln(\frac{P_{cyc}}{(a+bP_{cyc})^{\frac{3}{2}}})}{\partial \ln(P_{cyc})} = \frac{\partial \ln(\frac{P_{cyc}}{(a+bP_{cyc})^{\frac{3}{2}}})}{\frac{\partial \ln(P_{cyc})}{\partial P_{cyc}}} = \frac{\frac{(a+bP_{cyc})^{\frac{3}{2}}}{P_{cyc}} * \frac{(a+bP_{cyc})^{\frac{3}{2}} - \frac{3}{2}bP_{cyc}(a+bP_{cyc})^{\frac{1}{2}}}{(a+bP_{cyc})^3}}{\frac{1}{P_{cyc}}} = 1 - \frac{3}{2}\frac{bP_{cyc}}{a+bP_{cyc}}$$

$$\text{Reaction order in MCH } = 1 - \frac{3}{2} * \frac{\sum_i \frac{K_{c,i}}{P_H^{x_i}}P_{cyc}}{1+K_HP_H+\sum_i \frac{K_{c,i}}{P_H^{x_i}}P_{cyc}} = 1 - \frac{3}{2}\sum_i \theta_{cyc,i} \qquad \text{(S3)}$$

The correctness of Eq. (S3) can be tested at two extreme cases, i.e., at conditions that deplete the surface of MCH-derived species and that saturate the surface with MCH-derived species. In the former case, the coverage term related to MCH-derived species becomes much smaller compared with those related to dihydrogen derived species and

empty sites (Eq. (S2)), and thus the rate would become proportional to P_{MCH}; in the latter case, the coverage related to MCH-derived species becomes much larger compared with those related to dihydrogen derived species and empty sites, and thus the rate would become proportional to $P_{MCH}^{-0.5}$. Both agree with the predictions from Eq. (S3). The fact that the MCH order approaches 1.0 at very high H_2 pressures is also in line with a limited number of data collected at 543−563 K, 0.8 kPa MCH, 3.0 MPa H_2 (MCH order 0.9−1.0, not shown).

Along similar lines, if the RDS changes (as we shall see in Sections S3.2−3.4 discussion) to unassisted, H*-assisted, H_2-assisted C−C bond cleavage or H*-addition to the ring-opened state, we can also derive such relations between the MCH reaction order and the total coverage by MCH-derived species, as we show in later sections.

Such a simple relation as shown in Eq. (S3) will generally help to strengthen the reliability of simulation parameters obtained from kinetic modeling, as it provides a good estimate of the relative magnitude of the adsorption equilibrium constant of hydrogen and the dehydrogenation equilibrium constants of hydrocarbon, especially when different models produce similar goodness of fits. As we discuss later, the reaction order in MCH-d_0 (co-reactant: H_2) was always 20−40% lower than that measured in MCH-d_{14} (co-reactant: D_2). This indicates that the total coverages surface intermediates derived from the deuterated MCH have approximately 20−40% lower than in the case of non-deuterated MCH, and by inference, smaller thermodynamic constants for the equilibrated C−H bond dissociation steps (lumped with release of hydrogen molecules) than the latter. In line with this, the EIE for these C−H bond breaking steps are predicted by statistical thermodynamics to exhibit a normal isotope effect typically in the range of 1−2. We further exploit this useful observation in more detail in later sections.

S3.1.3. Prediction of isotope effects for H_2 activation, hydrocarbon dehydrogenation and rate determining C−H bond dissociation

a) IE on H_2/D_2 chemisorption (no translation or rotation for adsorbed H(D)-species):

(a-1):

$$(\frac{Q_H}{Q_D})_{trans} = (\frac{m_{D_2}}{m_{H_2}})^{3/2} = \frac{1}{(0.5)^{3/2}} = 2.83 \quad \text{(S4)}$$

(a-2):

$$(\frac{Q_H}{Q_D})_{rot} = \frac{\frac{1}{B_D}}{\frac{1}{B_H}} = \frac{60.9}{30.45} = 2 \quad \text{(S5)}$$

(a-3):

$$(\frac{Q_H}{Q_D})_{vib} = \frac{[(\frac{1-\exp(-hv_{Ir-D,A}/k_BT)}{1-\exp(-hv_{Ir-H,A}/k_BT)})(\frac{1-\exp(-hv_{Ir-D,E}/k_BT)}{1-\exp(-hv_{Ir-H,E}/k_BT)})^2]^2}{((\frac{1-\exp(-hv_{D_2}/k_BT)}{1-\exp(-hv_{H_2}/k_BT)})} = 0.44 \text{ (T = 523 K)}$$

(S6)

(a-4):

$$(\frac{Q_H}{Q_D})_{elec} = \exp([-2(ZPE_{Ir-H} - ZPE_{Ir-D}) + (ZPE_{H_2} - ZPE_{D_2})]/RT) = 0.49 \text{ (T = 523 K)}$$

(S7)

b) IE on lumped quasi-equilibrated C−H bond dissociation steps (surface species assumed to be immobile without any degrees of translational and rotational freedom):

(b-1):

$$(\frac{Q_{c,H}}{Q_{c,D}})_{trans} = \frac{[(\frac{m_{H_2}}{m_{D_2}})^{3/2}]^x}{(\frac{m_{C_7H_{14}}}{m_{C_7D_{14}}})^{3/2}} = \frac{[(\frac{2}{4})^{3/2}]^2}{(\frac{98}{112})^{3/2}} = 0.153 \, (x = 2) \quad \text{(S8)}$$

(b-2):

$$(\frac{Q_{c,H}}{Q_{c,D}})_{rot} = \frac{(\frac{B_{D_2}}{B_{H_2}})^x}{(\frac{I_{x,C_7H_{14}}}{I_{x,C_7D_{14}}} \times \frac{I_{y,C_7H_{14}}}{I_{y,C_7D_{14}}} \times \frac{I_{z,C_7H_{14}}}{I_{z,C_7D_{14}}})^{1/2}}$$

$$< \frac{(\frac{B_{D_2}}{B_{H_2}})^x}{(\frac{m_H}{m_D}\times\frac{m_H}{m_D}\times\frac{m_H}{m_D})^{1/2}} = \frac{(\frac{30.45}{60.9})^2}{(\frac{1}{2}\times\frac{1}{2}\times\frac{1}{2})^{1/2}} = 0.71\,(x=2) \quad \text{(S9)}$$

As the moments of inertia are all larger for deuterated species than for protiated ones, this ratio should be larger than $(\frac{B_{D_2}}{B_{H_2}})^x$, defining 0.25 as the lower boundary at x = 2. In asymmetric molecules, the moments of inertia about three mutually orthogonal axes x, y, and z with the origin at the center of mass of the system ($I_{x,y,z}$) are different from each other, defining 0.71 as the upper bound at x = 2.

We obtained the rotational partition functions for gaseous MCH-d_0 and -d_{14} at 523 K by means of theoretical calculations (Gaussian 09, Ver.02, B3LYP/6-311g (d,p), chair conformation) to obtain a more accurate estimate of that ratio. The value of $Q_{rot,MCH}$ is 4.8×10^5 (axial -CH_3) and 5.3×10^5 (equatorial -CH_3) for MCH-d_0, and 7.1×10^5 (axial -CH_3) and 7.6×10^5 (equatorial -CH_3) for MCH-d_{14}. Thus, the overall ratio of $(\frac{Q_{c,H}}{Q_{c,D}})_{rot}$ is:

$$(\frac{Q_{c,H}}{Q_{c,D}})_{rot} = \frac{(\frac{B_{D_2}}{B_{H_2}})^2}{\frac{Q_{rot,MCH-d0}}{Q_{rot,MCH-d14}}} = \frac{(\frac{30.45}{60.9})^2}{\frac{5.3\times10^5}{7.6\times10^5}} = 0.36 \quad \text{(S10)}$$

(b-3):

$$(\frac{Q_{c,H}}{Q_{c,D}})_{vib} = \frac{(\frac{Q_{C_7H_{14-2x}}}{Q_{C_7D_{14-2x}}})_{vib}[(\frac{Q_{H_2}}{Q_{D_2}})_{vib}]^x}{(\frac{Q_{C_7H_{14}}}{Q_{C_7D_{14}}})_{vib}}) = [(\frac{Q_{H_2}}{Q_{D_2}})_{vib}]^x \frac{(\frac{Q_{C_7H_{14-2x}}}{Q_{C_7H_{14}}})_{vib}}{(\frac{Q_{C_7D_{14-2x}}}{Q_{C_7D_{14}}})_{vib}} \quad \text{(S11)}$$

The vibrational partition functions of surface species (or those of the gas-phase reactant MCH-d_0 or -d_{14}) are not known. We can estimate, however, with a reasonably good accuracy, how much change is caused by dehydrogenation to the vibrational partition functions of both MCH-d_0 and MCH-d_{14}. The first term on the right-hand side of Eq. (S11) is unity as both vibrational frequencies for H_2 and D_2 appear at wavenumbers > 2900 cm^{-1}, and thus, the overall ratio would only depend on the second term, which can

be assessed as follows:

$$1 < \frac{(\frac{Q_{C_7H_{14-2x}}}{Q_{C_7H_{14}}})_{vib}}{(\frac{Q_{C_7D_{14-2x}}}{Q_{C_7D_{14}}})_{vib}} < 3.4 \text{ (T = 523 K)} \quad \text{(S12)}$$

This term is larger than unity because of the greater losses of vibrational entropies for deuterated species upon dehydrogenation. The upper boundary (3.4) reflects that the ultimate decrease (i.e., losing all the 42 C−H(D) vibrational degrees of freedom), upon dehydrogenation, in the value of vibrational partition function for gaseous reactant is 2.4 times greater for deuterated reactant than for the protiated counterpart. To a first approximation, if 12 C−H(D) vibrational degrees of freedom are lost (i.e., dehydrogenation depth $x = 2$), this ratio would be approximately $(3.4)^{12/42} \approx 1.44$.

(b-4):

$$(\frac{Q_{c,H}}{Q_{c,D}})_{elec} = \exp([2x(ZPE_{C-H} - ZPE_{C-D}) - x(ZPE_{H-H} - ZPE_{D-D})]/RT) = 29$$

(T = 523 K, $x = 2$) (S13)

Note that the ZPE difference between C−H and C−D bond in this case should take into account the ZPE differences of all the lost C−H(D) vibrations, as the detached H(D) atoms no longer exist in the intermediates. Using vibrational frequencies for cyclohexane-d_0 and -d_{12} listed in Table S1, we obtain:

ΔZPE (summed over 36 C−H or C−D vibrations) = ½ h($\Sigma\nu_{C-H}$ - $\Sigma\nu_{C-D}$) = 93.6 kJ mol^{-1}

Though it is not possible to isolate an individual frequency for each hydrogen, since the two hydrogens in the methylene group will couple, we can assume that three vibrations are associated with each C−H(D) bond. Therefore, the average ZPE difference between C−H and C−D bond after complete detachment of H(D) atoms is ca. 7.8 ± 0.2 kJ mol^{-1}.

Taking into account the separately treated partition functions, the IE on lumped quasi-equilibrated C−H bond dissociation steps is 0.153×0.36×1.44×29 = 2.2.

In the above treatment, we assumed that the average dehydrogenation depth is $x = 2$ for the sake of argument. Other pre-set values for x (0.5−4.0) lead to consistently high IE values for the quasi-equilibrated C−H bond dissociation steps (Table S3).

c) IE on the intrinsic rate constant

(c-1):

$$(\frac{Q_{rds,H}}{Q_{rds,D}})_{trans} \approx 1 \quad \text{(S14)}$$

(c-2):

$$(\frac{Q_{rds,H}}{Q_{rds,D}})_{rot} \approx 1 \quad \text{(S15)}$$

(c-3):

$$(\frac{Q_{rds,H}}{Q_{rds,D}})_{vib} \approx 1 \quad \text{(S16)}$$

(c-4):

In the case of a homolytic C−H bond cleavage without formation of Ir−H bond, a late transition state where the C−H(D) bond is significantly cleaved would lead to:

$$(\frac{Q_{rds,H}}{Q_{rds,D}})_{elec} = \exp([(ZPE_{C-H} - ZPE_{C-D})]/RT) = 3.1 \,(\text{T} = 523 \text{ K}) \quad \text{(S17)}$$

Note that ZPE difference here was taken as 4.9 kJ mol^{-1}, different from the chosen value of ZPE difference for predicting the isotope effects involved in the equilibrated C−H(D) activation (see above), as only one vibrational mode of the C−H(D) bond was lost during the formation of transition state. Earlier transition states would lead to smaller IEs. Moreover, the partial formation of Ir−H(D) bond in the transition state would also lead to smaller IEs. Thus, a more accurate expression of this term should reflect the ZPE differences for both C−H(D) bond breaking and Ir−H(D) bond formation processes:

$$(\frac{Q_{rds,H}}{Q_{rds,D}})_{elec} = \exp([x(ZPE_{C-H} - ZPE_{C-D}) - y(ZPE_{Ir-H} - ZPE_{Ir-D})]/RT) \quad \text{(S18)}$$

where *x* and *y* indicates the extent of bond breaking or formation, respectively.

To obtain a reliable estimate of the actual ZPE change toward arriving at the transition state for the C−H(D) bond dissociation, it is important to understand the measured KIEs for methane activation in methane activation on Ir (k_{CH4}/k_{CD4} = 1.8 at 873 K [S7]). From the first-order rate constants (0.6 s^{-1}) and activation energies (~ 80 kJ mol^{-1}), the entropy loss for the dissociative adsorption of methane-d_0 is predicted to be -100 J mol^{-1} K^{-1}, corresponding to two thirds of the translational entropy (160 J mol^{-1} K^{-1}) calculated from

its partition function. Therefore, we surmise that the measured KIE should reflect this consideration and is therefore a combination of translation and electronic partition function ratios. As a result, the ZPE change from the initial state to the transition state can be calculated from the following equation, using reported values of KIE:

$$KIE = [(\frac{m_{CD_4}}{m_{CH_4}})^{\frac{3}{2}}]^{\frac{2}{3}} \times \exp(\Delta ZPE_{TS-IS} / RT) \quad \text{(S19)}$$

The ZPE change estimated from the Eq. (S19) is 2.6−2.9 kJ mol^{-1}, much smaller than 4.9 kJ mol^{-1}, which clearly indicates that the kinetic isotope effect for C−H(D) bond breaking is attenuated from its upper bound value as a result of non-complete cleavage of the C−H(D) bond and partial formation of the Ir−H(D) bond in the TS. We applied this ZPE change to the present case (MCH, 523 K) and obtained a KIE on the RDS (C−H(D) bond breaking in the adsorbed intermediate) of 1.9.

d) Overall IE

In light of the rate expression, Eq. (S2), the overall IE for Group I mechanisms is:

$$IE_I = \frac{k_{rds,H}\theta_{cyc,rds,H}\theta_{\#,H}^{\frac{1}{2}}}{k_{rds,D}\theta_{cyc,rds,D}\theta_{\#,D}^{\frac{1}{2}}} = \frac{k_{rds,H}}{k_{rds,D}}\frac{K_{c,rds,H}}{K_{c,rds,D}}(\frac{1+K_DP_D+\sum_i \frac{K_{c,i,D}P_{cyc}}{P_D^{x_i}}}{1+K_HP_H+\sum_i \frac{K_{c,i,H}P_{cyc}}{P_H^{x_i}}})^{\frac{3}{2}} \quad \text{(S20)}$$

On small particles, the reaction order in MCH-d_0 in H_2 was 0.53 ± 0.03, while the order in MCH-d_{14} in D_2 was 0.67 ± 0.01 at 523 K, 0.9−1.6 kPa MCH and 0.64 MPa H_2/D_2 (Fig. S3). From Eq. (S3), the total coverage by MCH-derived species would be 0.31 ± 0.02 in the case of protiated reactants, and 0.22 ± 0.01 in the case of deuterated reactants. On large particles, the total coverage by MCH-derived species would be 0.50 ± 0.01 in the case of protiated reactants, and 0.40 ± 0.01 in the case of deuterated reactants at the conditions indicated above.

As shown above, the EIE on the dehydrogenation equilibrium constant varies with the dehydrogenation depth (x); it varies from 1.8 to 2.2 (immobile species) and from 1.5 to 1.8 (2D gas-like species) when x increases from 0.5 to 2.0. Correspondingly, the ratio of

$\frac{1+K_D P_D+\sum_i \frac{K_{c,i,D} P_{cyc}}{P_D{}^{x_i}}}{1+K_H P_H+\sum_i \frac{K_{c,i,H} P_{cyc}}{P_H{}^{x_i}}}$ varies within 0.70 ± 0.10 (immobile species) and 0.84 ± 0.10 (2D gas-like species) on small Ir particles, while it varies within 0.62 ± 0.09 (immobile species) and 0.74 ± 0.09 (2D gas-like species) on large particles.

Taken together, the predicted IE for this type of mechanism (Eq. (S20)) should be **2.3 ± 0.3** on small Ir particles and **1.9 ± 0.2** on large particles at 523 K, 0.9−1.6 kPa MCH and 0.64 MPa H_2/D_2. They are inconsistent with the measured values (1.8 on small particles, < 1.4 on large particles); any attempts to adjust the separate IEs to their respective lower or upper bound values do not lead to overall IEs close to the measured ones within experimental uncertainties. From the above analyses, this type of mechanistic proposals can be discarded as responsible for endocyclic hydrogenolysis reactions.

S3.2. Group I mechanisms-variant I': the first C–H bond cleavage as the RDS

S3.2.1. Derivation of rate expression for Group I mechanisms-variant I'

The first C–H(D) bond cleavage can also be the rate-determining step. This scenario, which is not included in the analysis made in Section S3.1, is to be discussed here. The sequence of steps is presented in Scheme S6.

(i) H_2 chemisorption (as in Scheme S4)

(ii) The first C–H bond cleavage being irreversible and rate-determining (the length of arrows shown below does not imply the relative magnitude of rate coefficients):

$c\text{-}C_7H_{14}\ (g) + 2^* \xrightarrow{k_1} c\text{-}C_7H_{13}^* + H^* \qquad r_1 = k_1 P_{cyc} \theta_*^2$

$c\text{-}C_7H_{13}^* + 2^* \xrightarrow{k_2} c\text{-}C_7H_{12}^{**} + H^* \qquad r_2 = k_2 \theta_{cyc} \theta_*^2$

... ... (kinetically insignificant)

(where θ_{cyc} is the coverage by the most abundant MCH-derived surface

intermediate, which in this case is assumed to be c-C_7H_{13}*)

Scheme S6. A schematic sequence for Group I Mechanism-variant I' which assumes quasi-equilibrated H_2 dissociation and the first C−H bond breaking step as rate-limiting. Kinetically insignificant steps are not shown.

Pseudo-steady-state-hypothesis (PSSH) applied to c-C_7H_{13}*:

$d[c\text{-}C_7H_{13}^*]/dt = r_1 - r_2 = 0$

(the reverse of the second C−H bond cleavage is assumed negligble)

So: $\theta(c\text{-}C_7H_{13}^*) = \frac{k_1 P_{cyc}}{k_2}$

Applying site balance equation to all the surface species (including vacant site) gives the coverage of vacant site:

$$\theta_* = \frac{1 - \frac{k_1 P_{cyc}}{k_2}}{K_H^{0.5} P_H^{0.5} + 1}$$

Replacing this term into the rate form of r_1, we have:

Rate expression for Group I mechanism-variant I" (c-$C_7H_{13}^*$ as the most abundant C-containing intermediates)

$$r_* = \frac{k_1 P_{cyc}(1 - \frac{k_1 P_{cyc}}{k_2})}{1 + K_H^{0.5} P_H^{0.5}} \qquad \text{(S21)}$$

Rate equation (S21) predicts the most negative order in H_2 as -0.5 (for paired H* species, this value is -1), which is clearly incompatible with the measured values exceeding -2.0 on small Ir clusters at most reaction conditions [S5]. Even on large particles, measured H_2 orders varied from less negative values (e.g., -0.5) to positive ones [S5], measured small reaction orders (0.1−0.4) in MCH and the large KIE on the rate constant k_1 are all in conflict with this mechanism. In this light, an effort is not made to estimate its associated isotope effect.

S3.3. Group II mechanisms: C–C bond cleavage as the RDS

S3.3.1. Rate equation for Group II mechanisms

A generalized kinetic sequence for Group II mechanisms is presented in Scheme S7 without showing kinetically insignificant steps following the RDS. In this group of mechanisms, a C–C bond cleavage step after a number of hydrogen atoms have been abstracted, by the surface metal atoms, from the reactant is assumed to control the hydrogenolysis kinetics. Similar as in Section S3.1, the vacant site pair (*−*) can be considered as the active ensemble (#) in the kinetic treatment.

(i) H_2 chemisorption (as in Scheme S4)

(ii) Hydrocarbon activation (lumped with recombination of H^* into gas phase H_2):

$$c\text{-}C_7H_{14}\ (g) + *{-}* \overset{K_{cyc}}{\rightleftharpoons} (c\text{-}C_7H_{14-2x})** + xH_2\ (g) \qquad K_{cyc} = \frac{\theta_{cyc} P_H^{\,x}}{P_{cyc}\theta_{**}}$$

(where θ_{cyc} and x are the coverage by MCH-derived surface intermediates and the respective depth of dehydrogenation, respectively)

(iii) C–C bond cleavage (rate-determining):

$$(c\text{-}C_7H_{14-2x})** + \text{`}\mathbf{S}\text{'} \xrightarrow{k_{rds}} (RO\text{-}C_7H_{14-2x'})** \qquad R_{rds} = k_{rds}\,\theta_{cyc}\,\theta_{s'}$$

(where $(RO\text{-}C_7H_{14-2x'})^{**}$ is a ring-opened state different from the cyclic state with the prefix 'c', in which x may, or may not, be equal to x'; x is the depth of dehydrogenation and '**S**' can be an empty site (*), an adsorbed hydrogen (H^*), molecular H_2, or even non-existent for non-assisted C–C bond scission; any potential release of sites previously covered by '**S**' is not shown on the product side)

Scheme S7. A generalized kinetic sequence for Group II Mechanisms that assume quasi-equilibrated nature of H_2 dissociation and the C−H bond dissociation steps preceding the rate determining C−C bond breaking. Kinetically insignificant steps following the RDS

are not shown.

We consider all the possible C−C bond cleavage pathways via intermediates of different dehydrogenation extents and reactivities in the C−C bond cleavage. The rate of this reaction is governed by the rate of the RDS (step (iii), Scheme S7), the form of which depends on the species 'S', co-present with the C-containing intermediate:

General rate expressions for Group II mechanisms:

(II-1) When the C−C bond cleavage is unassisted (no 'S')

$$r_{*-*} = \sum_i k_{rds,II-1}\theta_{cyc,rds} = \frac{\sum_i k_{rds,II-1,i}\frac{K_{c,i}P_{cyc}}{P_H{}^{x_i}}}{1+K_H P_H+\sum_i \frac{K_{c,i}P_{cyc}}{P_H{}^{x_i}}} \quad \text{(S22)}$$

(II-2) When the species involved in the C−C bond cleavage is an adsorbed vicinal H-adatom ('S' = H):

$$r_{*-*} = \sum_i k_{rds,II-2}\theta_{cyc,rds}\theta_H = \frac{\sum_i k_{rds,II-2,i}\frac{K_{c,i}P_{cyc}}{P_H{}^{x_i}}(K_H P_H)^{0.5}}{(1+K_H P_H+\sum_i \frac{K_{c,i}P_{cyc}}{P_H{}^{x_i}})^{\frac{3}{2}}} \quad \text{(S23)}$$

(II-3) When the species involved in the C−C bond cleavage is a H_2 molecule ('S' = H_2):

$$r_{*-*} = \sum_i k_{rds,II-3}\theta_{cyc,rds}P_H = \frac{\sum_i k_{rds,II-3,i}\frac{K_{c,i}P_{cyc}}{P_H{}^{x_i}}P_H}{1+K_H P_H+\sum_i \frac{K_{c,i}P_{cyc}}{P_H{}^{x_i}}} \quad \text{(S24)}$$

Similar to the relation derived as Eq. (S3), the reaction order in MCH (n_{MCH}) can also be expressed as a function of the total coverage of MCH-derived intermediates in the above cases, respectively as:

$$n_{MCH} = 1-\sum_i \theta_{cyc,i} \quad \text{(no 'S')} \quad \text{(S25)}$$

$$n_{MCH} = 1 - \frac{3}{2}\sum_i \theta_{cyc,i} \quad (\text{'S'} = \text{H*}) \tag{S26}$$

$$n_{MCH} = 1 - \sum_i \theta_{cyc,i} \quad (\text{'S'} = \text{H}_2) \tag{S27}$$

The different subgroups of mechanism give rise to the following overall isotope effects, correspondingly as:

$$IE_{II-1} = \frac{\sum_i k_{rds,II-1,i,H} \dfrac{K_{c,i,H}}{P_H^{\,x_i}}}{\sum_i k_{rds,II-1,i,D} \dfrac{K_{c,i,D}}{P_D^{\,x_i}}} \left(\frac{1 + K_D P_D + \sum_i \dfrac{K_{c,i,D} P_{cyc}}{P_D^{\,x_i}}}{1 + K_H P_H + \sum_i \dfrac{K_{c,i,H} P_{cyc}}{P_H^{\,x_i}}}\right) \quad \text{(no 'S')} \tag{S28}$$

$$IE_{II-2} = \frac{\sum_i k_{rds,II-2,i,H} \dfrac{K_{c,i,H}}{P_H^{\,x_i}} K_H^{\,0.5}}{\sum_i k_{rds,II-2,i,D} \dfrac{K_{c,i,D}}{P_D^{\,x_i}} K_D^{\,0.5}} \left(\frac{1 + K_D P_D + \sum_i \dfrac{K_{c,i,D} P_{cyc}}{P_D^{\,x_i}}}{1 + K_H P_H + \sum_i \dfrac{K_{c,i,H} P_{cyc}}{P_H^{\,x_i}}}\right)^{\frac{3}{2}} \quad (\text{'S'} = \text{H*}) \tag{S29}$$

$$IE_{II-3} = \frac{\sum_i k_{rds,II-3,i,H} \dfrac{K_{c,i,H}}{P_H^{\,x_i}}}{\sum_i k_{rds,II-3,i,D} \dfrac{K_{c,i,D}}{P_D^{\,x_i}}} \left(\frac{1 + K_D P_D + \sum_i \dfrac{K_{c,i,D} P_{cyc}}{P_D^{\,x_i}}}{1 + K_H P_H + \sum_i \dfrac{K_{c,i,H} P_{cyc}}{P_H^{\,x_i}}}\right) \quad (\text{'S'} = \text{H}_2) \tag{S30}$$

The boundary values for these IEs can be determined, respectively, as follows, Eqs. ((S31)−(S33)):

$$\frac{k_{rds,II-1,i,H}}{k_{rds,II-1,i,D}} \left(\frac{K_{c,i,H}}{K_{c,i,D}}\right)_{\min} \left(\frac{1 + K_D P_D + \sum_i \dfrac{K_{c,i,D} P_{cyc}}{P_D^{\,x_i}}}{1 + K_H P_H + \sum_i \dfrac{K_{c,i,H} P_{cyc}}{P_H^{\,x_i}}}\right) < IE_{II-1} < \frac{k_{rds,II-1,i,H}}{k_{rds,II-1,i,D}} \left(\frac{K_{c,i,H}}{K_{c,i,D}}\right)_{\max} \left(\frac{1 + K_D P_D + \sum_i \dfrac{K_{c,i,D} P_{cyc}}{P_D^{\,x_i}}}{1 + K_H P_H + \sum_i \dfrac{K_{c,i,H} P_{cyc}}{P_H^{\,x_i}}}\right) \tag{S31}$$

$$\frac{k_{rds,II-2,i,H}}{k_{rds,II-2,i,D}} \left(\frac{K_H}{K_D}\right)^{0.5} \left(\frac{K_{c,i,H}}{K_{c,i,D}}\right)_{\min} \left(\frac{1 + K_D P_D + \sum_i \dfrac{K_{c,i,D} P_{cyc}}{P_D^{\,x_i}}}{1 + K_H P_H + \sum_i \dfrac{K_{c,i,H} P_{cyc}}{P_H^{\,x_i}}}\right)^{\frac{3}{2}} < IE_{II-2} < \frac{k_{rds,II-2,i,H}}{k_{rds,II-2,i,D}} \left(\frac{K_H}{K_D}\right)^{0.5} \left(\frac{K_{c,i,H}}{K_{c,i,D}}\right)_{\max} \left(\frac{1 + K_D P_D + \sum_i \dfrac{K_{c,i,D} P_{cyc}}{P_D^{\,x_i}}}{1 + K_H P_H + \sum_i \dfrac{K_{c,i,H} P_{cyc}}{P_H^{\,x_i}}}\right)^{\frac{3}{2}} \tag{S32}$$

$$\frac{k_{rds,II-3,i,H}}{k_{rds,II-3,i,D}} \left(\frac{K_{c,i,H}}{K_{c,i,D}}\right)_{\min} \left(\frac{1 + K_D P_D + \sum_i \dfrac{K_{c,i,D} P_{cyc}}{P_D^{\,x_i}}}{1 + K_H P_H + \sum_i \dfrac{K_{c,i,H} P_{cyc}}{P_H^{\,x_i}}}\right) < IE_{II-3} < \frac{k_{rds,II-3,i,H}}{k_{rds,II-3,i,D}} \left(\frac{K_{c,i,H}}{K_{c,i,D}}\right)_{\max} \left(\frac{1 + K_D P_D + \sum_i \dfrac{K_{c,i,D} P_{cyc}}{P_D^{\,x_i}}}{1 + K_H P_H + \sum_i \dfrac{K_{c,i,H} P_{cyc}}{P_H^{\,x_i}}}\right) \tag{S33}$$

(S33)

S3.3.2. Prediction of isotope effects for Group II mechanisms

For a given case (II-1 to II-3), the KIE on the rate constant for cleavage of an endocyclic C−C bond should be similar for any intermediate. For case (II-1), it should be close to unity as isotope identity ought not to affect the activation barrier. For case (II-2), the KIE is taken as 1.2−1.4 for a relatively early TS with slightly smaller ZPE difference than in the intial state [S8], or as 0.7−0.8 (calculated from the ZPE difference in Table 2, main text) for a late TS with surface Ir-H(D) bond nearly broken and C−H(D) nearly formed. For case (II-3), the KIE should reflect, in addition to the TS structure, the loss of some translational (rotational, vibrational) entropies of gas-phase $H_2(D_2)$ toward the formation of TS, but the exact value cannot be reliably estimated; the lower bound (> 1.7) is related to the loss of one degree of translational freedom for $H_2(D_2)$ and an early TS where H−H(D−D) is slightly stretched. A late TS where H−H(D−D) is nearly broken and C−H(D) is almost formed leads to even larger values (> 2.7), according to the ZPE differences (ΔZPE = 7.6−4.9 = 2.7 kJ mol^{-1}).

Since $k_{rds,II-1,i,H} \approx k_{rds,II-1,i,D}$ and $1.8 \leq \frac{K_{c,i,H}}{K_{c,i,D}} \leq 2.2$ (x = 0.5–2.0), and it is estimated, from the measured reaction orders in MCH-d_0 and -d_{14} on small and large particles, that the magnitude of the term $\frac{1+K_D P_D+\sum_i \frac{K_{c,i,D} P_{cyc}}{P_D{}^{x_i}}}{1+K_H P_H+\sum_i \frac{K_{c,i,H} P_{cyc}}{P_H{}^{x_i}}}$ is 0.60–0.80 for D_{Ir} = 0.52−0.65 and 0.51–0.71 for D_{Ir} =0.04–0.24 (Section S3.1.3d), the range of IE for mechanism (II-1) is determined to be 1.1–1.8 (D = 0.52−0.65) and 0.9–1.6 (D = 0.04–0.24).

Along similar lines, the range of IEs for mechanisms (II-2) and (II-3) can be determined by using Eqs. (S31)−(S33). The overall IEs estimated for each subgroup of mechanism, case (II-1) to (II-3), respectively, are summarized as follows:

Case (II-1): **1.1–1.8** (D = 0.52−0.65) or **0.9–1.6** (D = 0.04–0.24)

Case (II-2): (a) **Early TS: 1.1−2.4** (D = 0.52−0.65) or **0.9−2.0** (D = 0.04–0.24); (b) **Late TS: 0.6−1.4** (D = 0.52−0.65) or **0.5−1.1** (D = 0.04–0.24)

Case (II-3): (a) **Early TS: > 1.9** (D = 0.52−0.65) or **> 1.6** (D = 0.04–0.24); (b) **Late TS: > 3.4** (D = 0.52−0.65) or **> 2.9** (D = 0.04–0.24) (note: one degree of translational freedom in H_2/D_2 is assumed to be lost; more entropy losses in the RDS increase further these values)

Likely, the reactivities of different surface intermediates differ greatly and there may exist one most reactive intermediate. In this case, the more reactive intermediate would impose a greater influence on the observed isotope effects. We have discussed the consequence in the main text (Section 4.2.2.1). We also note that significantly inverse EIEs (e.g., 0.6 [S9]) on dihydrogen dissociation, instead of a normal one (1.2, Section S3.1.3a), would afford overall IEs smaller than observed, predicting Case II-2 (that involves an adsorbed H(D) atom in the RDS) to be unlikely regardless of the transition state structure.

S3.4. Group III mechanisms: C–H bond re-formation after C–C bond cleavage as the RDS

S3.4.1. Rate equation for Group III mechanisms

A generalized kinetic sequence for Group III mechanisms is presented in Scheme S8 without showing kinetically insignificant steps following the RDS. In this group of mechanisms, a certain step after the cleavage of the C–C bond in the reactant is assumed to control the hydrogenolysis kinetics.

(i) H_2 chemisorption (as in Scheme S4)

(ii) Lumped quasi-equilibrated steps before the RDS:

$$c\text{-}C_7H_{14}\,(g) + *\text{–}* \overset{K_{ro}}{\rightleftharpoons} (RO\text{-}C_7H_{14\text{-}2y})^{**} + yH_2\,(g) \qquad K_{ro} = \frac{\theta_{ro} P_H{}^{y}}{P_{cyc}\theta_{**}}$$

(where $(RO\text{-}C_7H_{14\text{-}2y})^{**}$ is a ring-opened state; K_{ro}, θ_{ro}, and y are the equilibrium constant for the formation of $(RO\text{-}C_7H_{14\text{-}2y})^{**}$ that appears in the RDS, the coverage by this species and its corresponding extent of dehydrogenation, respectively)

(iii) C–H bond re-formation (rate-determining):

$(RO\text{-}C_7H_{14-2y})^{**} + H^* \xrightarrow{k_{rds}} (RO\text{-}C_7H_{15-2y})^{**} + *$ $\quad R_{rds} = k_{rds}\,\theta_{ro}\,\theta_H$

Scheme S8. A generalized kinetic sequence for Group III Mechanisms which assume quasi-equilibrated nature of H_2 dissociation, C−H bond dissociation and C−C bond breaking steps preceding the rate determining C−H bond re-formation.

Similar as in Section S3.1, the vacant site pair (*−*) can be considered as the active ensemble (#) in the kinetic treatment. The rate of this reaction is governed by the rate of the RDS (step (iii), Scheme S8) and thus can be expressed as:

General rate expression for Group III mechanisms:

$$r_{*-*} = k_{rds,III}\theta_{ro,rds}\theta_H = \frac{k_{rds,III}\dfrac{K_{ro}P_{cyc}}{P_H^{\,y}}(K_H P_H)^{0.5}}{(1+K_H P_H+\sum_i \dfrac{K_{c,i}P_{cyc}}{P_H^{\,x_i}})^{\frac{3}{2}}} \tag{S34}$$

S3.4.2. Prediction of isotope effects for Group III mechanisms

The corresponding isotope effect is (assuming that the nature of the species appearing in the RDS, characterized by the value of *y*, does not change with isotope identity):

$$IE_{III} = \frac{k_{rds,III,H}K_{ro,H}K_H^{\,0.5}}{k_{rds,III,D}K_{ro,D}K_D^{\,0.5}}\left(\frac{1+K_D P_D+\sum_i \dfrac{K_{c,i,D}P_{cyc}}{P_D^{\,x_i}}}{1+K_H P_H+\sum_i \dfrac{K_{c,i,H}P_{cyc}}{P_H^{\,x_i}}}\right)^{\frac{3}{2}} \tag{S35}$$

The RDS for this type of mechanisms, which is the addition of a hydrogen adatom to one of the surface-bound carbon atoms in the ring-opened state, can be seen as an elementary step reverse to, and that shares the same transition state with (i.e., microscopic reversibility), the dissociation of a C−H(D) bond in a chemisorbed alkane. The ZPE difference in the initial state (Ir−H/Ir−D) is 3.5 kJ mol^{-1}, while that in the TS is 2.0−2.3 kJ mol^{-1} (see the main text). Accordingly, the KIE on the rate constant can be calculated

from the change of ZPE difference from the initial state to the TS:

$$(\frac{Q_{rds,H}}{Q_{rds,D}})_{elec} = \exp([\Delta ZPE_{IS} - \Delta ZPE_{TS})]/RT) = 1.3-1.4 \text{ (T = 523 K)} \quad \text{(S36)}$$

Using the average values estimated in the foregoing sections for $\frac{K_{ro,H}}{K_{ro,D}}$ (2.1), $\frac{K_H}{K_D}$ (1.2) and $\frac{1+K_D P_D + \sum_i \frac{K_{c,i,D} P_{cyc}}{P_D^{x_i}}}{1+K_H P_H + \sum_i \frac{K_{c,i,H} P_{cyc}}{P_H^{x_i}}}$ (0.60−0.80 on small particles; 0.51−0.71 on large particles), the overall IE for this type of mechanism is estimated to be **1.5−2.0** on small Ir clusters (D = 0.52–0.65) and **1.3−1.8** on large ones (D = 0.04−0.24). They agree with the observed values, within the uncertainties in experimental measurements. *If dihydrogen dissociation features a significantly inverse IE (0.6)*, which has sometimes been reported [S9], the IE would become **ca. 1.0 and 0.8**, respectively, on small and large particles, rendering this mechanism rather unlikely.

S3.5. Group IV mechanism: the 'multiplet' mechanism [S10]

In the 'multiplet' mechanism, the cyclic hydrocarbon is physically adsorbed over metal surfaces in a flat-lying and non-dissociating fashion; the ring is cleaved upon the attack of a co-adsorbed hydrogen atom [S10]. This mechanistic consideration leads to the following rate equation:

$$r = k_{rds} K_{phys} P_{cyc} \theta_H = \frac{k_{rds} K_{phys} P_{cyc} K_H^{0.5} P_H^{0.5}}{1+K_H^{0.5} P_H^{0.5}} \quad \text{(S37)}$$

In the first place, this rate equation provides a poor precision of describing the rate data on both small and large Ir particles [S5]. Furthermore, the IE predicted from this rate equation is:

$$IE_{IV} = \frac{k_{rds,H} K_{phys,H} K_H^{0.5}}{k_{rds,D} K_{phys,D} K_D^{0.5}} \frac{1+K_D^{0.5} P_D^{0.5}}{1+K_H^{0.5} P_H^{0.5}} \quad \text{(S38)}$$

Physisorption leads to some loss of translational freedom, the partition function of which

differs slightly between H- and D-containing species (1.14 for a loss of two degrees of translational freedom). The EIE on the coverage of chemisorbed hydrogen atoms is in the range of 1.0−1.1. The KIE on the k_{rds}, which involves the H*-assisted C−C bond cleavage, is thought to vary from small normal values (~ 1.3) to inverse ones (< 1.0), depending on the lateness of transition state. Therefore, the overall IE should be typically smaller than 1.5, in contradiction with the observed values on small clusters. Preliminary experiments with MCH-d_0+D_2 mixtures showed that the H-atoms in MCH-d_0 were extensively exchanged by D-atoms from D_2 in great excess (Fig. S4), an impossible scenario for the direct cleavage mechanism without surface dehydrogenation steps preceding.

S3.6. Plausible pathways for exocyclic hydrogenolysis

Exocyclic hydrogenolysis exhibited slightly larger IEs than endocyclic hydrogenolysis on high dispersion catalysts, while showing much larger IEs on low-dispersion catalysts. Two potential mechanisms may account for the large IE values (> 4 for the lowest dispersion studied). One invokes a C−H(D) bond dissociation step as the RDS, while the other proposes a mobile hydrogen adatom involved in the RDS.

If C−H(D) bond dissociation becomes rate limiting during exocyclic hydrogenolysis turnovers on very large particles (D = 0.035), the expression of the overall IE would resemble Eq. (S20). Its value should be the product of the terms, shown in Eq. (S20), $1.9 \times 2.9 \times (0.71)^{1.5} = 3.3$.

The very large IE and the increasing trend with increasing particle size can be rationalized by increasing participation of a mobile hydrogen species in the rate determining step as particle size grows. Its presence has been suggested in many studies on hydrogenation and hydrogenolysis reactions [S11−S13]. After the definition of ‘mobile’ species by Eyring et al. [S14], such hydrogen adatoms lose one degree of translational freedom normal to the surface. Split hydrogen atoms have no rotational entropy. Their vibrational frequencies appear at high wavenumbers around or above 2000 cm^{-1} [S15–S18]. Using reported frequencies for weakly held Rh−H and Pt−H species and standard expressions of partition functions, the EIE on the coverage of such hydrogen atoms are estimated to be 2.8−3.2. If one such mobile hydrogen atom is involved in the

rate-determining step−be it cleavage of the exocyclic C−C bond or re-formation of a certain C−H(D) bond after the ring is opened−we can envisage a large overall IE as observed on low-dispersion catalysts.

Appendix S1

The entire set of surface reactions for dihydrogen are, in the most rigorous form:

$H_2 + *\text{-}* = H*\text{-}H*$ K_1

$H*\text{-}H* = H* + H*$ K_2

$H_2 + * + * = H* + H*$ K_3

Summation of the three equation gives 2* = *-*, which expresses the expectation that adsorption equilibrium of dihydrogen allows for the interchange of pair sites with individual sites. Therefore, we have:

$$\theta_{H*-H*} = K_1 P_{H_2} \theta_{*-*}$$
$$(\theta_{H*})^2 = K_2 \theta_{H*-H*}$$
$$(\theta_{H*})^2 = K_3 P_{H_2} (\theta_*)^2$$

The coverages of individual empty site and empty site pairs are related by the following:

$$\theta_{*-*} = Z(\theta_*)^2$$

Putting the factor Z, which is a probability factor of finding neighboring vacancy, into the intrinsic equilibrium constant, the coverages of H* and H*-H* are in a functional form of $(K_H P_H)^{0.5}$ and $(K_{H,pair} P_H)^1$, respectively, both relative to the coverage of paired empty sites (*-*). These considerations would lead to a more complex equation, Eq (S1') in Section S3.1.1. However, we did not base our discussion on the exact functional form of the rate equation; instead, Eq (S3) shows that the measured order in MCH and surface coverage of hydrocarbon species are correlated, circumventing the need for a knowledge of the functional form of hydrogen coverage.

References

[S1] G. Parkin, Acc. Chem. Res. 42 (2009) 315.

[S2] J. Au-Yeung, K.D. Chen, A.T. Bell, E. Iglesia, J. Catal. 188 (1999) 132.

[S3] A. Ozaki, Isotopic Studies of Heterogeneous Catalysis, Academic Press, New York, 1977.

[S4] M. Ojeda, A.-W. Li, R. Nabar, A.U. Niekar, M. Mavrikakis, E. Iglesia, J. Phys. Chem. C 114 (2010) 19761.

[S5] H. Shi, O.Y. Gutiérrez, G.L. Haller, D. Mei, R. Rousseau, J.A. Lercher, J. Catal. 297 (2013) 70.

[S6] H. Shi, X.B. Li, G.L. Haller, O.Y. Gutiérrez, J.A. Lercher, J. Catal. 295 (2012) 133.

[S7] J.M. Wei, E. Iglesia, Phys. Chem. Chem. Phys. 6 (2004) 3754.

[S8] H. Wang, E. Iglesia, J. Catal. 273 (2010) 245.

[S9] H. Wang, E. Iglesia, ChemCatChem. 3 (2011) 1166.

[S10] O.V. Bragin, A.L. Liberman, Uspekhi Khimii 39 (1970) 21.

[S11] K.A. Son, J.L. Gland, J. Am. Chem. Soc. 118 (1996) 10505.

[S12] S.T. Ceyer, Acc. Chem. Res. 34 (2001) 737.

[S13] K.L. Haug, T. Bürgi, T.R. Trautman, S.T. Ceyer, J. Am. Chem. Soc. 120 (1998) 8885.

[S14] S. Glasstone, K.J. Laidler, H. Eyring, The Theory of Rate Processes, McGraw-Hill, NY, 1941.

[S15] S. M. Davis, W. D. Gillespie, G. A. Somorjai, J. Catal. 83 (1983) 131.

[S16] A. M. Baro, H. D. Bruchman, H. Ibach, Surf. Sci. 88 (1979) 384.

[S17] J. P. Candy, P. Fouilloux, M. Primet, Surf. Sci. 72 (1978) 167.

[S18] J. P. Wey, W. C. Neely, S. D. Worley, J. Phys. Chem. 95 (1991) 8881.

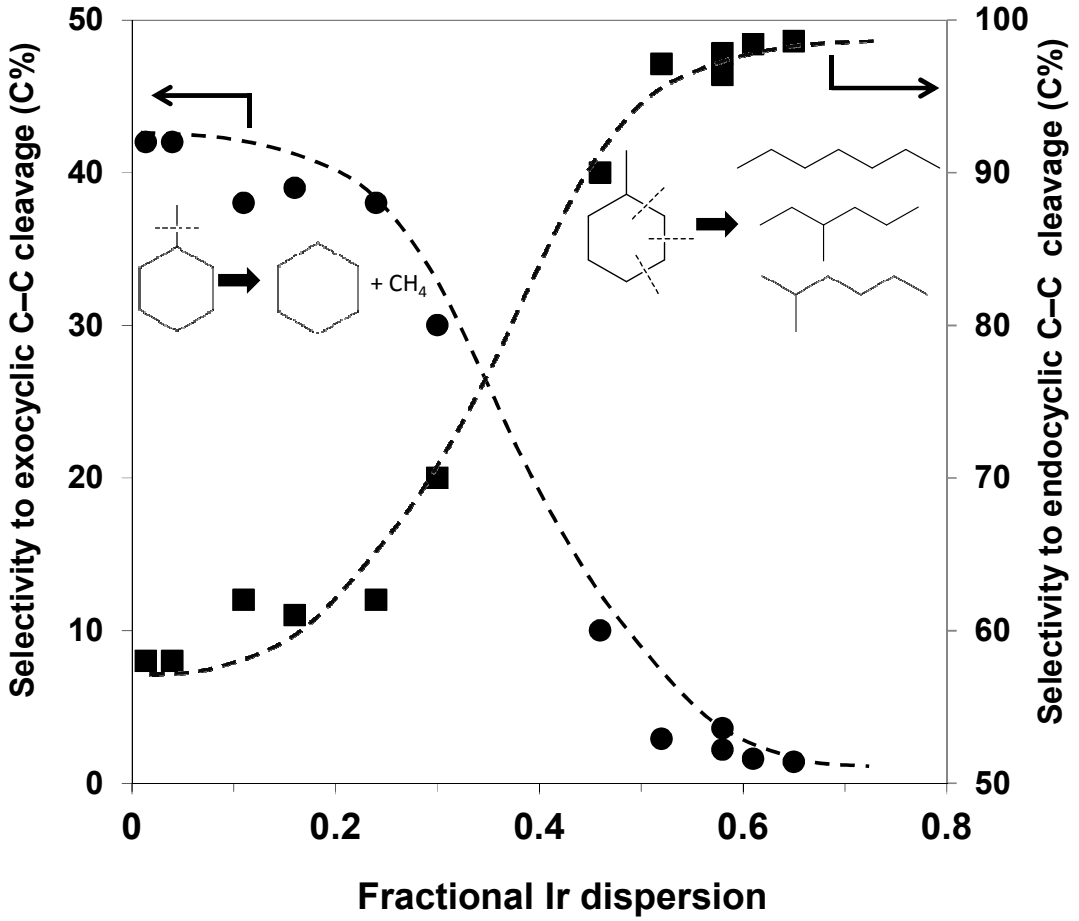

Figure S1. The dependence of the endocyclic (■) and exocyclic (●) C–C bond cleavage on the Ir dispersion in the hydrogenolysis of MCH on Ir black and Ir/Al_2O_3 catalysts at T = 523 K, 1.2 kPa MCH and 0.37 MPa H_2. The selectivity limits at low and high Ir dispersions vary with temperature and reactant pressures. These results were reported and analyzed in Ref. [S5].

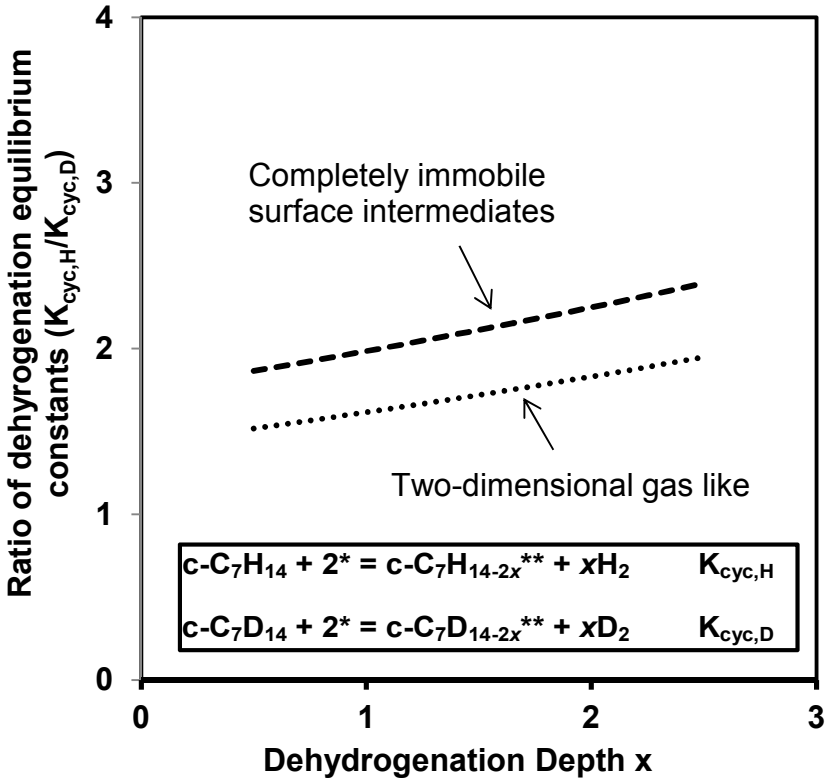

Figure S2. The dependence of the theoretically assessed ratio of dehydrogenation equilibrium constant (the inset rectangle) on the dehydrogenation depth (x). The dashed lines indicate the different assumptions for the surface intermediates: 'completely immobile' means no translational or rotational degrees of freedom are retained in the surface species; 'two-dimensional gas like' means the surface intermediates have 2 degrees of translational freedom and 1 degree of rotational freedom (rotation about the C−C bond bound to the surface).

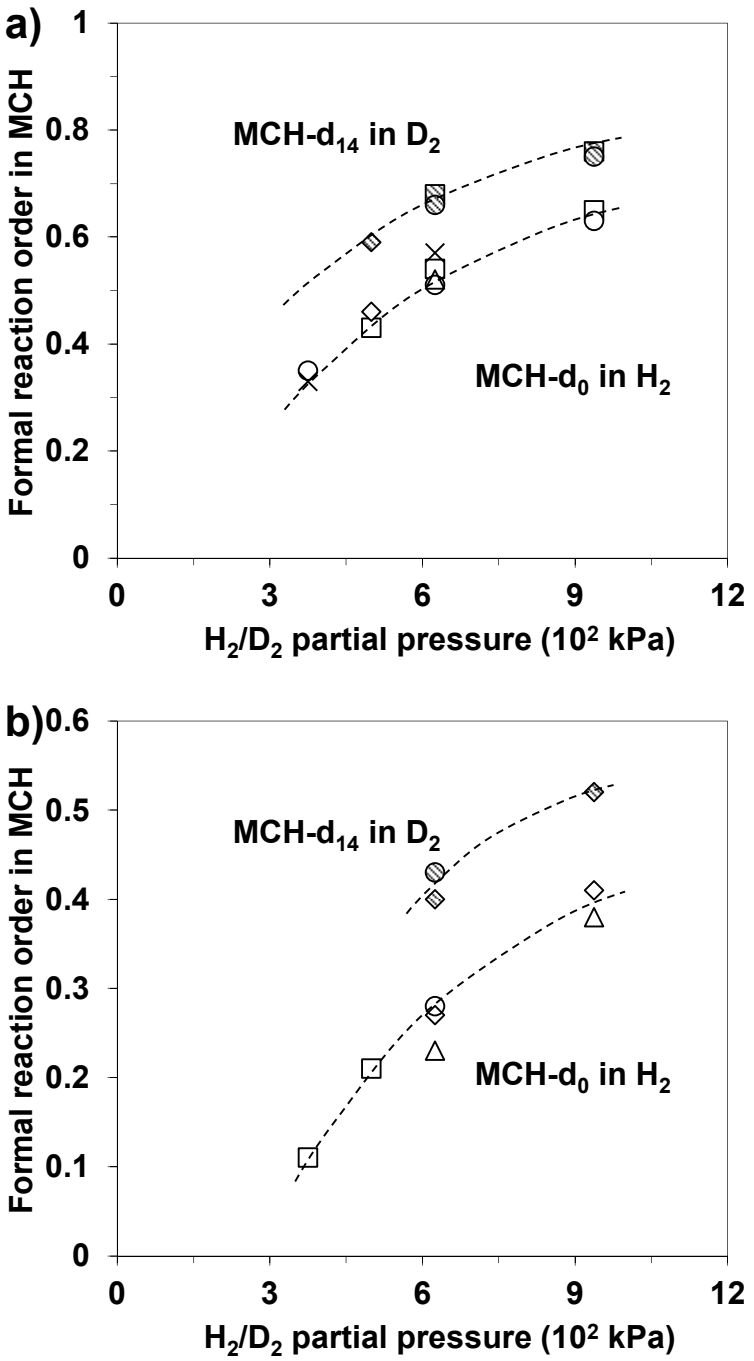

Figure S3. Formal reaction order in MCH-d_0 (i.e., $\frac{\partial \ln(r_{endocyclic})}{\partial \ln(P_{MCH})}$) as a function of H_2/D_2 pressure on (a) small (D > 0.50) and (b) large (D < 0.20) Ir particles at 523 K and 0.9−1.6 kPa MCH. Different symbols represent catalysts with different dispersions within each group.

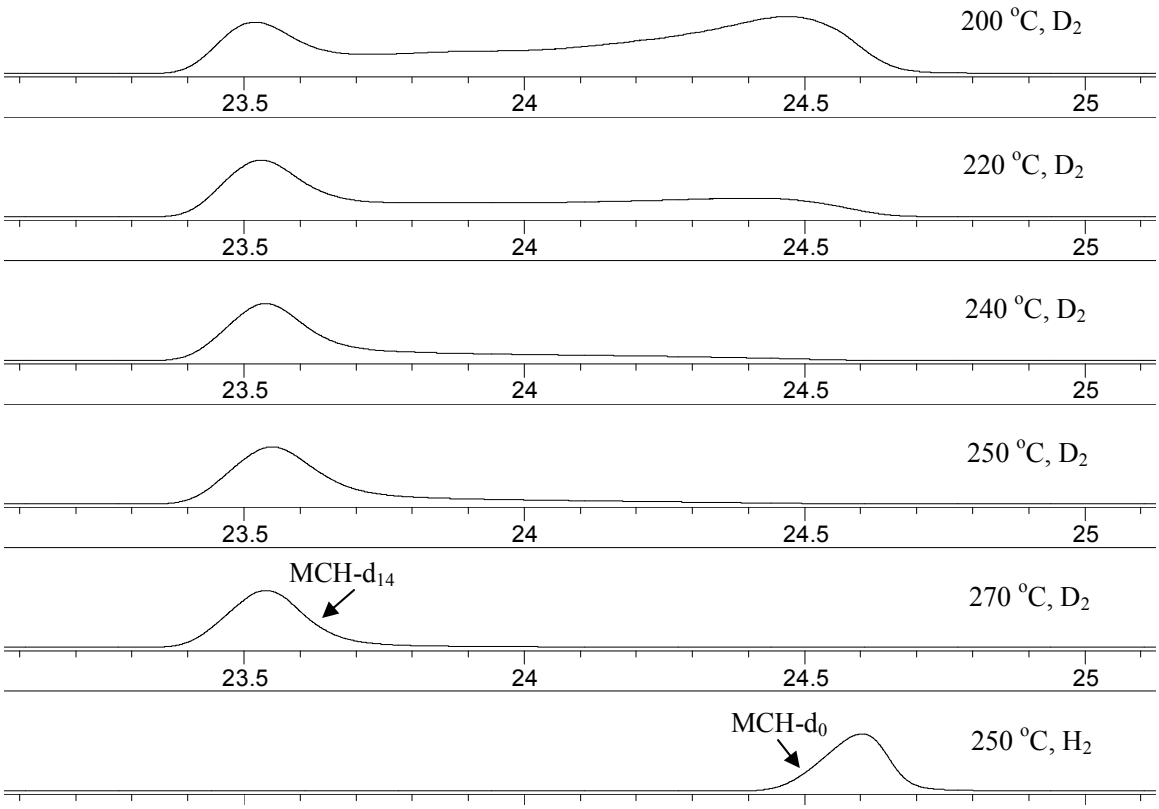

Figure S4. Representative GC profiles for the reaction of MCH-d_0 in dihydrogen on Ir catalysts at different temperatures (dihydrogen/MCH-d_0 ratio > 100).

Table S1 Vibrational frequencies (cm^{-1}) related to vibrational modes of C−H bonds (i.e., C−C bond vibrations not included) in cyclohexane and cyclohexane-d_{12}. Data from: T. Shimanouchi, Tables of Molecular Vibrational Frequencies Consolidated Vol. I, National Bureau of Standards, 1972, 1.

$c\text{-}C_6H_{12}$			$c\text{-}C_6D_{12}$		
Type of mode	Value (cm^{-1})	Degeneracy	Type of mode	Value (cm^{-1})	Degeneracy
CH_2 a-str[a]	2930[g]	1	CD_2 a-str[a]	2152[h]	1
CH_2 s-str[a]	2852[g]	1	CD_2 s-str[a]	2082[h]	1
CH_2 scis[a]	1465[h]	1	CD_2 scis[a]	1117[h]	1
CH_2 rock[a]	1157[h]	1	CD_2 rock[a]	1012[h]	1
CH_2 twist[b]	1383[h]	1	CD_2 twist[b]	864[g]	1
CH_2 wag[b]	1157[h]	1	CD_2 wag[b]	842[g]	1
CH_2 wag[c]	1437[h]	1	CD_2 wag[c]	1126[g]	1
CH_2 twist[c]	1090[h]	1	CD_2 twist[c]	778[g]	1
CH_2 a-str[d]	2915[g]	1	CD_2 a-str[d]	2206[h]	1
CH_2 s-str[d]	2860[g]	1	CD_2 s-str[d]	2108[h]	1
CH_2 scis[d]	1437[h]	1	CD_2 scis[d]	1091[k]	1
CH_2 rock[d]	1030[i]	1	CD_2 rock[d]	917[j]	1
CH_2 a-str[e]	2930[g]	2	CD_2 a-str[e]	2199[h]	2
CH_2 s-str[e]	2897[g]	2	CD_2 s-str[e]	2104[h]	2
CH_2 scis[e]	1443[h]	2	CD_2 scis[e]	1071[h]	2
CH_2 wag[e]	1347[h]	2	CD_2 wag[e]	1212[h]	2
CH_2 twist[e]	1266[h]	2	CD_2 twist[e]	937[h]	2
CH_2 rock[e]	785[h]	2	CD_2 rock[e]	637[h]	2
CH_2 a-str[f]	2933[j]	2	CD_2 a-str[f]	2206[h]	2
CH_2 s-str[f]	2863[j]	2	CD_2 s-str[f]	2108[h]	2
CH_2 scis[f]	1457[j]	2	CD_2 scis[f]	1069[h]	2
CH_2 wag[f]	1355[k]	2	CD_2 wag[f]	1165[j]	2

CH_2 twist[f]	1261[j]	2	CD_2 twist[f]	991 [j]	2
CH_2 rock[f]	907[k]	2	CD_2 rock[f]	687[k]	2

[a] Symmetry a_1g.
[b] Symmetry a_1u.
[c] Symmetry a_2g.
[d] Symmetry a_2u.
[e] Symmetry eg.
[f] Symmetry eu.
[g] 15~30 cm^{-1} uncertainty.
[h] 3~6 cm^{-1} uncertainty.
[i] 6~15 cm^{-1} uncertainty.
[j] 0~1 cm^{-1} uncertainty.
[k] 1~3 cm^{-1} uncertainty.

Table S2 Vibrational partition function at T = 523 K (Q_{vib}) related to vibrational modes of C−H bonds (i.e., C−C bond vibrations not included) in cyclohexane and cyclohexane-d_{12}.

c-C_6H_{12}		c-C_6D_{12}	
Type of mode[a]	$Q_{vib,i} = \frac{1}{1-\exp\left(\frac{-h\nu_i}{k_B T}\right)}$	Type of mode[a]	$Q_{vib,i} = \frac{1}{1-\exp\left(\frac{-h\nu_i}{k_B T}\right)}$
CH_2 a-str	1.000	CD_2 a-str	1.003
CH_2 s-str	1.000	CD_2 s-str	1.003
CH_2 scis	1.018	CD_2 scis	1.048
CH_2 rock	1.043	CD_2 rock	1.065
CH_2 twist	1.022	CD_2 twist	1.101
CH_2 wag	1.043	CD_2 wag	1.108
CH_2 wag	1.019	CD_2 wag	1.047
CH_2 twist	1.052	CD_2 twist	1.132
CH_2 a-str	1.000	CD_2 a-str	1.002
CH_2 s-str	1.000	CD_2 s-str	1.003
CH_2 scis	1.019	CD_2 scis	1.052
CH_2 rock	1.062	CD_2 rock	1.086
CH_2 a-str	1.001[b]	CD_2 a-str	1.005[b]
CH_2 s-str	1.001[b]	CD_2 s-str	1.006[b]
CH_2 scis	1.038[b]	CD_2 scis	1.113[b]
CH_2 wag	1.050[b]	CD_2 wag	1.074[b]
CH_2 twist	1.063[b]	CD_2 twist	1.169[b]
CH_2 rock	1.275[b]	CD_2 rock	1.460[b]
CH_2 a-str	1.001[b]	CD_2 a-str	1.005[b]
CH_2 s-str	1.001[b]	CD_2 s-str	1.006[b]
CH_2 scis	1.037[b]	CD_2 scis	1.113[b]
CH_2 wag	1.049[b]	CD_2 wag	1.085[b]
CH_2 twist	1.064[b]	CD_2 twist	1.144[b]

CH_2 rock	1.186[b]	CD_2 rock	1.385[b]
	Overall $Q_{\text{vib}} = \prod_{i}^{i} Q_{vib,i}$		Overall $Q_{\text{vib}} = \prod_{i}^{i} Q_{vib,i}$
	2.681		7.451

[a] Exactly corresponding to the wavenumber and degeneracy in Table S1.
[b] The Q_{vib} has been squared due to the double degeneracy (E_u or E_g) of these modes.

Table S3 Estimated ratios of partition functions $(Q_{C,H}/Q_{C,D})_{trans,rot,vib,elec}$ for quasi-equilibrated C−H(D) bond dissociation steps (c-C_7H_{14} + 2* = c-C_7H_{14-2x}** + xH_2) at 523 K. Surface species are assumed to be either immobile without any degrees of translational and rotational freedom or completely mobile as the gas phase molecules.

Dehydrogenation depth (x)	$Q_{C,H}/Q_{C,D}$			
	Translational	Rotational	Vibrational	Electronic
0.5[a]	0.726 (immobile) 0.594 (mobile)	1.05 (immobile) 0.71 (mobile)	1.09	2.3
1.0	0.432 (immobile) 0.353 (mobile)	0.74 (immobile) 0.50 (mobile)	1.20	5.3
1.5	0.257 (immobile) 0.210 (mobile)	0.52 (immobile) 0.353 (mobile)	1.30	12.4
2.0	0.153 (immobile) 0.125 (mobile)	0.36 (immobile) 0.25 (mobile)	1.44	28.1
2.5[b]	0.091 (immobile) 0.074 (mobile)	0.26 (immobile) 0.18 (mobile)	1.58	66.5
3.0[b]	0.054 (immobile) 0.047 (mobile)	0.18 (immobile) 0.12 (mobile)	1.71	153.9
4.0[b]	0.019 (immobile) 0.017 (mobile)	0.09 (immobile) 0.06 (mobile)	2.04	825.0

[a] For the sake of comparison, the number of surface atoms needed to bind the intermediates is still assumed to be two in this case, while it is not conceptually sound to cleave only one C−H(D) bond and bind two C atoms to two surface Ir atoms.

[b] For the sake of comparison, the number of surface atoms needed to bind the intermediates is still assumed to be two in this case; however, it is not conceptually sound to cleave more than four endocyclic C−H bonds, as the maximum number of bonds between an Ir atom and an endocyclic C (already linked to two C atoms) is two. Deeper dehydrogenation has to be achieved by adsorption modes (e.g., α,γ-adsorption, flat adsorption) that enable the contact of other carbon atoms with the surface.